Nonlinear Dynamic States' Estimation and Prediction Using Polynomial Predictive Modeling Estimation et prédiction d'états dynamiques non linéaires à l'aide d'une modélisation prédictive polynomiale

Dileep Sivaraman, *Graduate Student Member, IEEE*, Songpol Ongwattanakul, *Member, IEEE*, Jackrit Suthakorn, *Member, IEEE*, and Branesh M. Pillai, *Member, IEEE*

***Abstract*— In motion-control applications, noise and dynamic nonlinearities influence the performance of control systems and lead to unpredictable disturbances. The dc servo motors used in motion control applications should have precise control methods to achieve the desired responses. Therefore, predicting and compensating for the disturbance are essential for increasing system robustness and achieving high precision and fast reaction. This article introduces the polynomial predictive filtering (PPF) method to estimate the states of a system using polynomial extrapolation of consecutive and evenly spaced sensor data. Acceleration-/torque-based experiments are conducted to validate the effectiveness and viability of the proposed method. The difference between the real-time sensor data and the PPF-based predicted value shows a standard deviation of less than 0.15 and 1×10^{-5} for the velocity and disturbance torque, respectively.**

***Résumé*— Dans les applications de contrôle des mouvements, le bruit et les non-linéarités dynamiques influencent les performances des systémes de contrôle et entraînent des perturbations imprévisibles. Les servomoteurs à courant continu utilisés dans les applications de contrôle des mouvements doivent faire l'objet de méthodes de contrôle précises pour obtenir les réponses souhaitées. Par conséquent, il est essentiel de prévoir et de compenser les perturbations afin d'accroître la robustesse du système et d'obtenir une grande précision et une réaction rapide. Cet article présente la méthode de filtrage prédictif polynomial (PPF) pour estimer les états d'un système en utilisant l'extrapolation polynomiale de données de capteurs consécutives et régulièrement espacées. Des expériences basées sur l'accélération et le couple sont menées pour valider l'efficacité et la viabilité de la méthode proposée. La différence entre les données du capteur en temps réel et la valeur prédite par la méthode PPF présente un écart type inférieur à 0,15 et 1×10^{-5} pour la vitesse et le couple perturbateur, respectivement.**

***Index Terms*— Disturbance observer (DOB), motion control, polynomial extrapolation, reaction torque observer (RTOB), state estimation.**

Nomenclature

I_a^{ref}	Reference current.
$\ddot{\theta}$	Angular acceleration of the motor.
T_f	Friction torque.
T_{dis}	Disturbance torque.
B	Damping viscous coefficient.
K_t	Motor constants.
K_{tn}	Nominal motor constants.
G_{dis}	Filter coefficient.
J_n	Nominal rotor inertia.
J	Rotor inertia.

Manuscript received 21 June 2022; revised 31 October 2022 and 26 January 2023; accepted 17 March 2023. Date of publication 8 June 2023; date of current version 7 July 2023. This work was supported by the Reinventing University: Mahidol Medical Robotics Platform Project through Mahidol University, Nakhon Pathom, Thailand, under Grant IO 864102063000. *(Corresponding author: Branesh M. Pillai.)*

The authors are with the Department of Biomedical Engineering, Center for Biomedical and Robotics Technology (BART LAB), Faculty of Engineering, Mahidol University, Nakhon Pathom 73170, Thailand (e-mail: branesh.mad@mahidol.ac.th).

Associate Editor managing this article's review: Jalal Habibi.

Digital Object Identifier 10.1109/ICJECE.2023.3260830

I. Introduction

Motion control techniques, which have been advanced intensely in the last few decades, play an indispensable role in many industrial automation applications [1], [2], [3]. The efficacy of the robotic application systems is predominantly centered on position and force control [4]. To accomplish precise position and torque control, dc servomotors are extensively employed. The dc servomotors are commonly used in robotics owing to their simple structure and significant testing efficiency at a low cost. The prediction of position, velocity, acceleration, force, and nonlinearities of such instruments are very important in robotic applications [5], [6].

Therefore, estimation and compensation of the disturbance are critical for increasing the system robustness and achieving high precision and fast reactions [7]. As unknown signals influence the performance of control systems and may contribute to disturbances, dynamic nonlinearities can cause disturbances in the system. A disturbance observer (DOB) is a tool for correcting disturbances that are particularly useful and commonly used in robotic motion control applications [8], [9], [10], [11]. The DOB, as the name implies, measures and estimates the disturbance. It compensates for unknown disturbances once they have been measured [12]. Owing to the compensation effect, the net effect on the system is a near-zero disturbance [13]. Control in disturbances must be estimated and predicted properly to obtain the desired response of the system, and its estimation depends on the errors of the sensor data from the systems.

However, these errors are intrinsic to any physical system. Nevertheless, measured data can be smoothed or filtered to reduce the effects of noise [14], [15]. These datasets are composed of samples from slowly fluctuating analog signals, which can be modeled as low-order polynomial segments [16]. When it comes to predicting future samples of such signals, this assumption comes in handy. Predictive filtering is useful in automatic control applications, where the delay in a feedback loop must be reduced to a minimum to ensure fast system controllability [17], [18], [19], [20].

In real-time applications, many industrial control systems do not allow for the inclusion of additional delays in the signal path. Kalman and α–β filters blend noisy and limited sensor readings to produce the best possible estimate of the state of the system. Moreover, such methods are computationally expensive [21]. The extended Kalman filter (EKF) requires more computation in each moderately dimensional state space. The EKF essentially entails utilizing a Taylor series expansion to linearize the model equations to the first order [22]. In addition, this method also has several limitations. First, only small nonlinearities can be accommodated when first-order approximation is sufficiently accurate. This necessitates computing the observation matrices and Jacobian of the state transition. Therefore, these algorithms may be complex and challenging to maintain as the model changes and also possible that the algorithm will diverge [23]. This article proposes the possibility of using low-degree polynomials to estimate and predict the states and motion control parameters of dc motors. This method can reduce computational expenses, and the mathematical burden and small nonlinearities can be accommodated by using a sufficiently accurate low-order polynomial approximation. However, the application of polynomial predictive filtering (PPF) was not limited to this domain. Further application areas can be classified as areas where a higher degree of polynomial filtering is required and areas where exceptionally fast execution speeds are required, such as plant control, inertial kinematics, and tracking [24], [25], [26].

Polynomial modeling is regarded as one of the most powerful tools for signal processing [27]. To approximate and predict data from motor drives, low-degree polynomials or sinusoids can be used. For example, the high inertia of the motor and load inhibits an abrupt stepwise increase in angular velocity. The practical velocity curves are always smooth, owing to the inertia. Smooth signals can be accurately described as low-degree polynomials within a limited time period [28]. Therefore, the angular velocity has been approximated using a low-degree polynomial in many practical scenarios [29], [30], [31], [32]. Hence, for the prediction of random signals and the separation of random signals from random noise, numerous studies have been conducted on the detection of signals of known form in the presence of random noise [33], [34], [35], [36]. The motivation of these studies is to develop a specification for a linear/nonlinear dynamic system that can predict, separate, or detect random signals, as described in Section III. For this purpose, the authors developed a numerical solution based on the polynomial modeling of sensor data to obtain future values from previous values. This research takes an alternative look at a set of issues, sidestepping the difficulties previously highlighted and avoiding computational expenses and the mathematical burden of using low-degree polynomial equations. In this study, a state estimator was developed with an accurate and precise estimation in the presence of uncertainty in the sensor data using polynomial extrapolation. In addition, the PPF predicts the forthcoming states based on previous sensor data.

The PPF algorithm works by a three-phase process: initialization is performed only once, and it provides the initial system state and initial state uncertainty, followed by the prediction. The state update process is responsible for the future state estimation of the system. In this phase, PPF requires measured value, measurement uncertainty, previous system state, and estimate uncertainty. Based on these inputs, the state update process calculates the gain and provides the predicted system state and the current state that estimate the uncertainty. In the second phase, the future values are predicted using polynomial extrapolation. The third phase (the prediction process) calculates the predicted system state, and the uncertainty of the current system state estimates the next system state based on the dynamic model of the system. For dc motor applications, the system state can be predicted using a lower degree polynomial equation. The viability of the proposed method was combined and analyzed using the observer-based dc motor parameter estimation method [1] described in Section IV. Acceleration-/torque-based experiments were also performed for the statistical analysis and validation of the proposed method.

II. Notation Conventions

We will mainly deal with discrete dynamic systems throughout the study; that is, signals will be observed at evenly spaced points in time. Small-hat letters indicate the values to be predicted ($\hat{z}$).

III. Modeling of Polynomial Predictive Filter

The one-degree polynomial extrapolation performs using two data points (which is also a linear extrapolation). Three data points are used to create a quadratic polynomial equation. Similarly, an $(m-1)$-degree polynomial requires m data points [37]. This study assumes that the signal can be modeled as an mth-order polynomial. However, forecasting future values of a primary signal affected by additive white Gaussian noise or uniformly distributed noise is a common problem [38]. Any measurement value is the result of a linear combination of signal value and measurement noise [39]. Both are considered to be Gaussian. Thus, the estimation of a future value of a signal from the past samples of a polynomial function can be written as

$$\hat{y} = \hat{z} + e \quad (1)$$

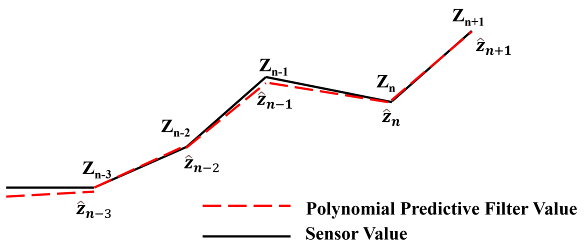

Fig. 1. Schematic of the proposed method.

where $\hat{z}$ is the estimated value of signal using polynomial extrapolation and e is the disturbing noise component. $\hat{z}$ can be calculated for consecutive and evenly spaced points as follows. If $z_1, z_2, z_3, \ldots, z_{n-2}, z_{n-1}, z_n, z_{n+1}, \ldots$ are the corresponding values of equally spaced and consecutive values of a polynomial function of x_i, and z_n is any value of $f(x_n)$, then

$$\hat{z}_n = \sum_{q=1}^{m+1} \frac{(-1)^{(q+1)}(m+1)!}{q![m-(q-1)]!} z_{(n-q)} \tag{2}$$

or

$$\hat{z}_n = \frac{(m+1)}{1!} z_{(n-1)} - \frac{m(m+1)}{2!} z_{(n-2)} + \cdots \tag{3}$$

where m is the degree of the polynomial, and $q = 1, 2, 3, \ldots, (m+1)$, $q < m+1$. Fig. 1 demonstrates a pictorial representation of the method.

For a two-degree polynomial

$$z_n = a x_n^2 + b x_n + c. \tag{4}$$

From (3) and (4), the nth value can be predicted from the previous value as

$$\hat{z}_n = 3z_{(n-1)} - 3z_{(n-2)} + z_{(n-3)}. \tag{5}$$

Proof: If the polynomial equation of mth-degree satisfies (2), it can be written as (6).

$$(x+y)^m = \sum_{q=1}^{p} \frac{(-1)^{(q+1)}(m+1)!}{q![m-(q-1)]!} (x+(y-q))^m \qquad [m-(q-1)] > 0. \tag{6}$$

Lemma 1:

$$\sum_{q=1}^{p} \frac{(-1)^{(q+1)}(m+1)!}{q![m-(q-1)]!} = 1 \qquad \{[m-(q-1)] > 0\} \quad \forall m \in \mathbb{N}. \tag{7}$$

Equation (7) can be expanded as

$$\frac{(m+1)}{1!} - \frac{m(m+1)}{2!} + \frac{m(m-1)(m+1)}{3!} \cdots = 1. \tag{8}$$

Proof of Lemma 1: Adding and subtracting 1 in the left-hand side of (8)

$$1 = \frac{(m+1)!}{(m+1)!}. \tag{9}$$

Equation (8) becomes

$$\begin{aligned}
&\frac{(m+1)!}{(m+1)!} - \frac{(m+1)}{1!} - \frac{m(m+1)}{2!} + \frac{m(m-1)(m+1)}{3!} + \cdots \\
&= 1 - \left[\binom{m+1}{0} + \binom{m+1}{1}(-1) + \binom{m+1}{2}(-1)^2 + \cdots \right] \\
&= 1 - (1-1)^{(m+1)} = 1.
\end{aligned}$$

Thus, according to (3) for an m-degree polynomial and by binomial theorem expansion

$$\begin{aligned}
&(x+(y+2))^m \\
&= \frac{(m+1)}{1!}(x+(y+1))^m - \frac{m(m+1)}{2!}(x+(y))^m + \cdots \\
&= \frac{(m+1)}{1!}[x^m + mx^{(m-1)}(y+1) + \cdots] - \frac{m(m+1)}{2!} \\
&\quad \times \left[x^m + mx^{(m-1)}y + \frac{m(m-1)}{2!} x^{(m-2)} y^2 + \cdots \right] \\
&\quad + \frac{m(m-1)(m+1)}{3!} \\
&\quad \times \left[x^m + mx^{(m-1)}(y-1) + \frac{m(m-1)}{2!} x^{(m-2)} (y-1)^2 + \cdots \right] \\
&= x^m \left[\frac{(m+1)}{1!} - \frac{m(m+1)}{2!} + \frac{m(m-1)(m+1)}{3!} \cdots \right] \\
&\quad + mx^{(m-1)} \left[\frac{(m+1)}{1!}(y+1) - \frac{m(m+1)}{2!} y + \cdots \right] \\
&\quad + \frac{m(m-1)}{2!} x^{(m-2)} \left[\frac{(m+1)}{1!}(y+1)^2 - \frac{m(m+1)}{2!} y^2 + \cdots \right] \\
&\quad + \frac{m(m-1)(m-2)}{3!} x^{(m-3)} \left[\frac{(m+1)}{1!}(y+1)^3 \right. \\
&\qquad\qquad \left. - \frac{m(m+1)}{2!} y^3 \cdots \right] \cdots \\
&= x^m + mx^{(m-1)}(y+2) + \frac{m(m-1)}{2!} x^{(m-2)} (y+2)^2 + \cdots .
\end{aligned} \tag{10}$$

Since

$$\frac{(m+1)}{1!} - \frac{m(m+1)}{2!} + \frac{m(m-1)(m+1)}{3!} \cdots = 1 \tag{11}$$

$$\frac{(m+1)}{1!}(y+1) - \frac{m(m+1)}{2!} y + \cdots = y+2 \tag{12}$$

$$\frac{(m+1)}{1!}(y+1)^2 - \frac{m(m+1)}{2!} y^2 + \cdots = (y+2)^2 \tag{13}$$

$$\frac{(m+1)}{1!}(y+1)^3 - \frac{m(m+1)}{2!} y^3 + \cdots = (y+2)^3 \tag{14}$$

which implies

$$(x+(y+2))^m = \frac{(m+1)}{1!}(x+(y+1))^m - \frac{m(m+1)}{2!}(x+y)^m + \cdots .$$

Hence, the following is proven:

$$\hat{z}_n = \sum_{q=1}^{p} \frac{(-1)^{(q+1)}(m+1)!}{q![m-(q-1)]!} z_{(n-q)} \tag{15}$$

where z_{n-q} represents the previous values of the polynomial functions. Assume a system whose state can measure in successive steps. If the system is static, one does not modify its state in a reasonable period of time. Therefore, multiple measurements can be taken and averaged

$$\hat{y}_{n,n} = \frac{1}{N}\sum_{n=1}^{N} z_n \tag{16}$$

where y is the true value, z_n is the measurement value at time n, and $\hat{y}_{n,n}$ is the estimate of y at time n (the estimate is made after taking the measurement z_{n-1}). Since the dynamic model is static, that is, the states do not change over time, therefore, $\hat{y}_{n+1,n} = \hat{y}_{n,n}$. Although the above equation is mathematically correct, it is impractical for implementation. To estimate $\hat{y}_{n,n}$, previous measurements must be remembered, particularly for states that change with time. If $\hat{y}_{n,n-1}$ is the previous estimate of y that was made at time $(n-1)$ (the estimate was made after taking the measurement z_{n-2}), $\hat{y}_{n+1,n}$ is the estimate of the future state $(n+1)$ of y. The estimate is made at the time n, right after the measurement z_n. In other words, $\hat{y}_{n+1,n}$ is a predicted state. From (1), the state update equation is given as follows:

$$\hat{y}_{n,n-1} = \hat{z}_n + G_n(\alpha_n - \hat{z}_n) = (1 - G_n)\hat{z}_n + G_n\alpha_n \tag{17}$$

where G_n is called the gain. The subscript n indicates that the gain can change with every iteration. The term $\hat{z}_n$ is a predicted value; it contains the new information and is calculated from previously measured values. α_n represents the value of system dynamics or the value calculated from the dynamic model of our system. The second part of (17) represents the measurement noise. Therefore, the value of the measurement noise should be estimated and updated at each iteration. Suppose that two devices with different designs to measure the measurements z_1^1 and z_1^2 are likely to be different from each other and from the actual value z_c. Ad hoc solution to this issue is given as [40]

$$y\left(z_1^1, z_1^2\right) = \beta * z_1^1 + \alpha * z_1^2. \tag{18}$$

The result of adding the two sensor values or the estimators z_1^1 and z_1^2 should be the same if they are equal. This suggests that $\beta + \alpha = 1$. Consequently,

$$y\left(z_1^1, z_1^2\right) = (1 - \alpha) * z_1^1 + \alpha * z_1^2. \tag{19}$$

Thus, the optimal linear estimator $y(z_1^1, z_1^2)$ from the Kalman filter is [34], [40]

$$y\left(z_1^1, z_1^2\right) = z_1^1 + K\left(z_1^2 - z_1^1\right) \tag{20}$$

where

$$K = \frac{\sigma_1^2}{\sigma_1^2 + \sigma_2^2} \tag{21}$$

where σ_1^2 and σ_2^2 are the variance of the measurements. By comparing (17) and (21)

$$\hat{z}_n + G_n(\alpha_n - \hat{z}_n) = z_1^1 + K\left(z_1^2 - z_1^1\right). \tag{22}$$

For a single-input–single-output (SISO) system $z_1^2 = \alpha_n$, it can be converted into an MISO system when α_n takes from another sensor data instead of dynamic model value

$$\hat{z}_n + G_n(\alpha_n - \hat{z}_n) = z_1^1 + K\left(\alpha_n - z_1^1\right). \tag{23}$$

If the sensor data can be modeled as a one-degree polynomial ($m = 1$, linear), then, from (3)

$$\hat{z}_n = 2z_{n-1} - z_{n-2}. \tag{24}$$

According to (2), for a nonlinear system

$$\hat{z}_n = \sum_{q=1}^{m+1} \frac{(-1)^{(q+1)}(m+1)!}{q![m-(q-1)]!} z_{(n-q)}. \tag{25}$$

A. Gain Equation

It is known that the true value, the estimated value, and the measured value may not always be equal. Measurement errors are the differences between measurements and true values. The measurement uncertainty (σ_m^2) is the variance in measurement errors. The variance of the measurement errors can be derived using a calibration procedure or by a scale vendor. The measurement error variance is the measurement uncertainty. The estimated error is the difference between the estimated and true values. The less precise our measurement is, the noisier it is. Noise or uncertainty is captured directly by variance. As a result, the lower the gain, the greater the measurement variance noise. The noisier our process state is, the more important innovation should be considered. As a result, the larger the process state variance, the greater the gain. Thus, the variance of a linear sum of two measurements is given as [41]

$$p_{n,n} = \frac{p_{n,n-1} r_n}{p_{n,n-1} + r_n} = p_{n,n-1} - \frac{p_{n,n-1}^2}{p_{n,n-1} + r_n}.$$

The gain factor G_n is given as

$$G_n = \frac{\text{Process Noise}}{\text{Process Noise} + \text{Measurement Noise}} \tag{26}$$

$$G_n = \frac{p_{n,n-1}}{p_{n,n-1} + r_n}. \tag{27}$$

$p_{n,n-1}$ is the extrapolated estimate uncertainty (uncertainty in estimate) and r_n is the measurement uncertainty.

B. Estimate Uncertainty Update

The gain is close to one when the measurement uncertainty is small and the estimated uncertainty is large. From (27), the estimate uncertainty update is defined as

$$p_{n,n} = (1 - G_n)p_{n,n-1}. \tag{28}$$

$p_{n,n}$ and $p_{n,n-1}$ are the estimated uncertainty of the current state and the estimated uncertainty that were calculated during the previous filter estimation, respectively. This equation updates the current state's estimated uncertainty. Since $(1 - G_n) < 1$, the equation that estimates uncertainty is always getting smaller with each filter iteration. When the measurement uncertainty is high, the gain is minimal, and the estimated uncertainty will take a long time to converge.

TABLE I
DC MOTOR SPECIFICATIONS

Specification of motors	
Manufacturer	Electrocraft
Version	E240
Maximum Terminal Voltage	60V DC
Supply Voltage	32V DC
Continuous stall Torque	20.5 Ncm
Peak Torque	169.5 Ncm
Maximum Speed	5000 rpm
Rotor Inertia	0.268 Kgcm2
Maximum Friction Torque	2.1 Ncm
Weight	1Kg
Torque Constant	13.5 Ncm/Amp
Terminal Resistance	5.4 Ω
Armature Inductance	8.2 mH

When the measurement uncertainty is small, however, the gain is large, and the estimated uncertainty quickly approaches zero. For a constant dynamic system, the estimated uncertainty extrapolation would be

$$p_{n+1,n} = p_{n,n}. \tag{29}$$

However, in a real situation, the system dynamic model contains uncertainty [42]. Thus, the process noise or model noise refers to the dynamic model's uncertainty. If the estimation errors are caused by process noise and the process noise variance is denoted by q, then the covariance extrapolation equation for constant dynamics is

$$p_{n+1,n} = p_{n,n} + q_n. \tag{30}$$

The initialization is executed only once, and it provides two parameters: the initial system state ($\hat{z}_{1,0}$) and the initial state uncertainty ($p_{1,0}$). However, another system or process can provide initialization parameters. The measurement is executed for every filter cycle and provides the measured system state (z_n) and measurement uncertainty (r_n). Fig. 2 provides a schematic description of the algorithm. The PPF can converge close to the true value even if the initialization parameters are not precise. The experimental results provide convincing evidence in favor of the convergence of PPF values to the true value, as described in Section IV.

IV. IMPLEMENTATION OF ALGORITHM

To validate the proposed method, we conducted an experiment to collect the data from the dc motor, as shown in Fig. 3. The motor's specifications are provided in Table I. A pulse width modulation (PWM)-based motor driver using a driver IC (DRV8432 by Texas Instrument) that can carry current up to 14 A with a peak load of 24 A drives the motor. The processor generates the PWM signals. To sense the position, an encoder is connected to the motor, and its specifications are provided in Table II. All computations are written in C and run on a real-time operating system (RTOS) with a 100-μs sample time.

The DOB is used as a torque sensor in this study, and the block diagram of the reaction DOB is shown in Fig. 4. DOB identifies the total mechanical load, and the influence of system parameter changes on the total motor disturbance.

TABLE II
ENCODER SPECIFICATIONS

Specification of encoder	
Model	H25D (BEI)
Pulse Count	2,500 ppr (pulse per revolution)
Pulse count with QEI	10,000 ppr
Supply Voltage	5 to 28 VDC available
Applied voltage	12 VDC
Current Requirements	100 mA, 250 mA (max)
Voltage/Output	28V/5: 5-28 VDC in, Vout= 5 VDC
Frequency Response	100 kHz, up to 1MHz
Moment of Inertia	5.2 X 10-4oz-in-sec2

The reaction torque T_{rec} can be measured if the frictional components are measured and eliminated from the disturbance output [43]. This is a reaction torque observer (RTOB), which is a variation of the DOB [7]. In the experiment, the rotor rotates for 30 s, and the velocity response of these rotations, total torque, and disturbance torque is measured. In this situation, a one-degree polynomial can be used to approximate the data from motor drives. If z_{n-1} and z_{n-2} are the DOB measurement values at times $(n-1)$ and $(n-2)$, respectively, use (24) to estimate the value of $\hat{z}_n$ (current time) from these previous values. Thus, the disturbance torque from (17) is given as

$$\hat{T}_{\text{dis}_n} = \hat{z}_n + G_n(\alpha_n - \hat{z}_n). \tag{31}$$

By comparing the DOB measurement values at nth time and the PPF value, the accuracy and efficiency of the proposed method can be estimated. To predict the $(n+1)$th time disturbance or predict the disturbance torque

$$\hat{z}_{n+1} = 2z_n - z_{n-1}. \tag{32}$$

From the above equation, $\hat{T}_{\text{dis}_{n+1}}$ can be forecast. This opens up a new way for us to use DOB data to predict the future values of the disturbance in the system. In other words, DOB can be converted into a predictor. In this experiment, a system dynamic equation to determine the value of the disturbance torque T_{dis} was obtained from [1]

$$\alpha_n = T_{\text{dis}} = K_{\text{tn}} I_a - J_n \dot{\omega} \tag{33}$$

where the torque coefficient is K_t, which can be calculated in the rotor stall test, and the inertia of the load linked with the rotor is J_n, which is calculated using three tests: the acceleration motion test, the deceleration motion test, and the reverse motion acceleration test. Nominal values are denoted by the subscript n. However, these values are always kept constant; therefore, compared to the DOB value, these values are less accurate. This produces fluctuations in the prediction. By considering this situation, to validate our model, we compared the values from the encoder and DOB values with the estimated value of the velocity and disturbance torque from the PPF estimator, respectively. Statistical analysis of the data is described in Section IV-A.

A. Statistical Analysis of PPF Model

This section summarizes the primary statistical modeling and analysis results associated with the PPF. Experiments were performed to demonstrate the importance and validity of all

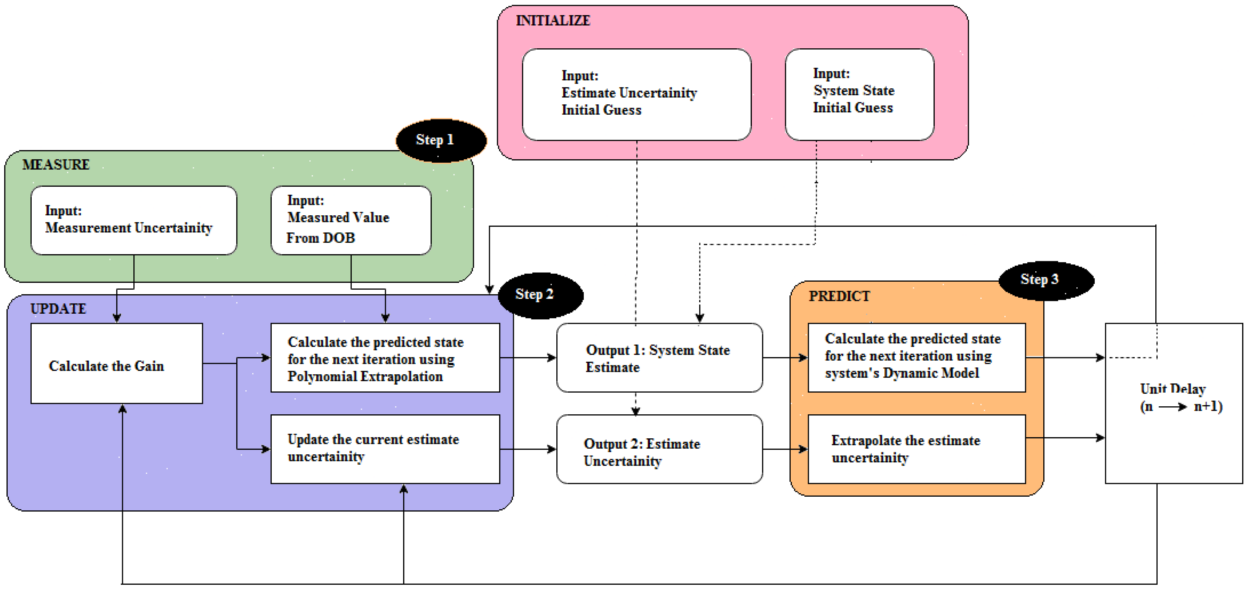

Fig. 2. Schematic description of the algorithm.

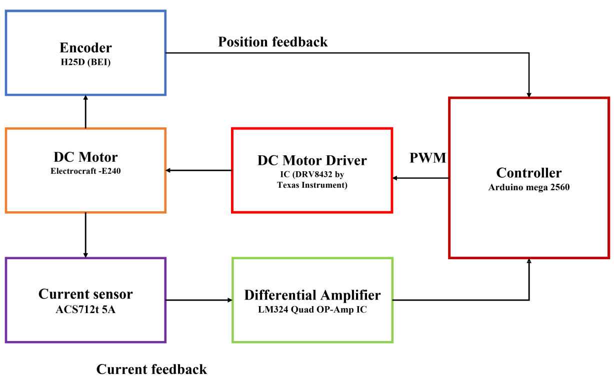

Fig. 3. Block diagram of the one-DOF rotational manipulator.

TABLE III
ANALYSIS OF MOTOR VELOCITY

Velocity (rpm)	Extrapolated Value		PPF Value	
	σ^2	σ	σ^2	σ
50	0.0159	0.1262	0.0131	0.1148
100	0.0188	0.1373	0.0157	0.1255
500	0.1940	0.4405	0.1619	0.4024

predicted values of the velocity and disturbance torque using the PPF. In addition, the predicted values were compared with the DOB data. The sample for this study consisted of three different velocities of a dc motor, and the relationship between the data from the sensor and the predicted values was analyzed. From the analysis, a correlation was found between the sensor data and predicted values.

In the experiment, the rotor rotated for 30 s and contained more than 1800 samples of sensor data. These data satisfy the one-degree polynomial extrapolation condition of (24). Since sensor data were precise; the process noise variance (q) is set to 0.0001, and the measurement error (standard deviation) was set to 0.1. Using (27), (28), and (30), it can calculate the values of gain and estimate the uncertainty, respectively. Variance and standard deviations were used to determine the correlation between the predicted and sensor data. The variance (σ^2) and standard deviation (σ) of the predicted values with the sensor data are illustrated in Table III. When analyzing the table, a minimum standard deviation of 0.12624 for the minimum velocity (50 rpm) was obtained, and it was clear that the predicted values were close to the sensor data. However, the standard deviations of the other two velocities (0.1373 and 0.4405) did not deviate significantly from the real value. In this study, two analyses were conducted, and the accuracy of the polynomial extrapolation model was initially determined. The second method determined the PPF model accuracy because the predicted samples contained Gaussian noise. Equation (1) shows the elimination of these values. The second result shows that the values of σ are smaller than those of the polynomial extrapolation model and very close to the real values. This means that the data error reduction occurred much better than polynomial extrapolation.

For the disturbance torque, the same experiment was repeated at three velocities in two different directions. The same accuracy test was conducted using the polynomial extrapolation model and PPF. Here, the most accurate value for the minimum velocity was obtained, which was negligible ($\sigma = 2.02 \times 10^{-6}$ for the extrapolation model and $\sigma = 2.02 \times 10^{-6}$ for PPF). Variance and standard deviation of the predicted values are illustrated in Table IV.

In addition to the variance and standard deviation values, 30 samples were plotted with the predicted values and sensor data, as shown in Figs. 5–7. The horizontal axis describes the time, whereas the vertical axis represents the velocity. Figs. 5–7 are a graphic summary of the relationship between the sensor data, extrapolated values, and PPF values. The sample for this study consisted of three different velocities

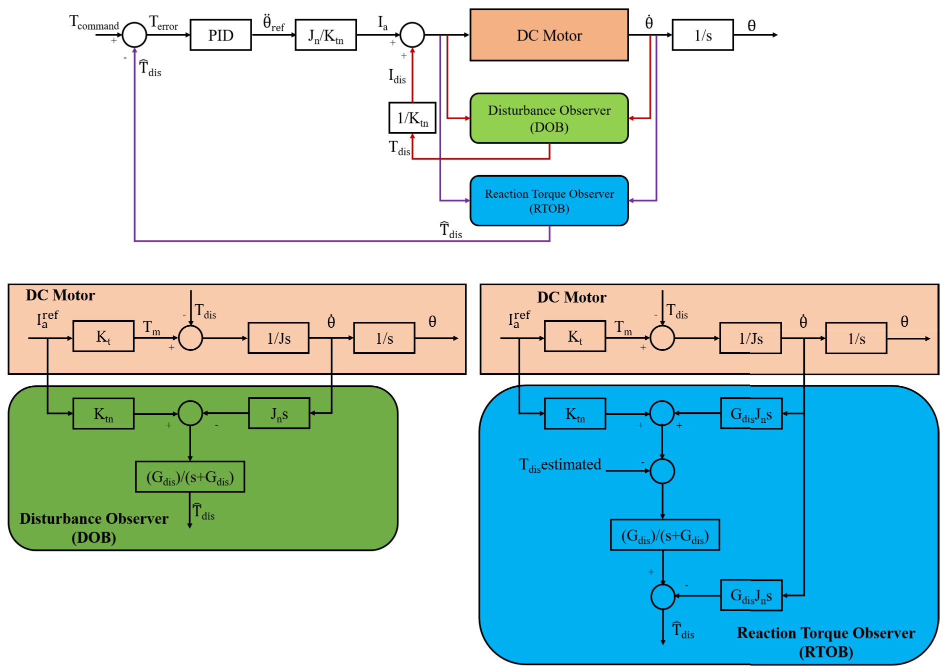

Fig. 4. DOB with the dc motor.

TABLE IV
ANALYSIS OF MOTOR DISTURBANCE TORQUE

Velocity (rpm)	Extrapolated Value		PPF Value	
	$\sigma^2(10^{-11})$	$\sigma(10^{-6})$	$\sigma^2(10^{-11})$	$\sigma(10^{-6})$
+50	0.41	2.02	0.33	1.83
-50	3.54	5.95	2.90	5.39
+100	0.39	1.99	0.32	1.80
-100	3.43	5.86	2.81	5.31
+500	2.27	4.77	1.86	4.32
-500	6.29	7.94	5.16	7.19

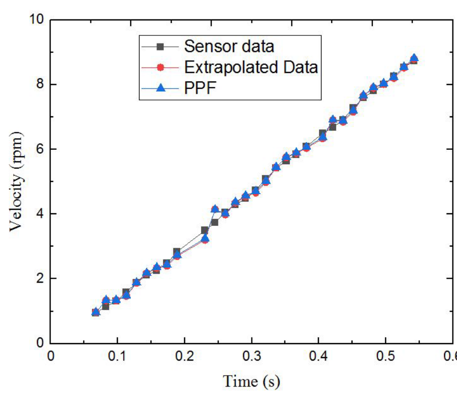

Fig. 5. 50-rpm velocity sensor data with extrapolated and PPF values.

(50, 100, and 500 rpm) of a dc motor, as shown in the figures. In the figures, the blue line indicates the PPF-predicted values from DOB's previous DOB values. The black lines are the real-time values obtained from the DOB. A minimum standard deviation of 0.11148 was obtained for PPF at a velocity of 50 rpm, and it is clear that the predicted values are close to the sensor data. However, the standard deviation of the other two velocities (0.1255 and 0.4024) did not deviate significantly from the real value. Our figure provides strong evidence of the accuracy of the PPF method.

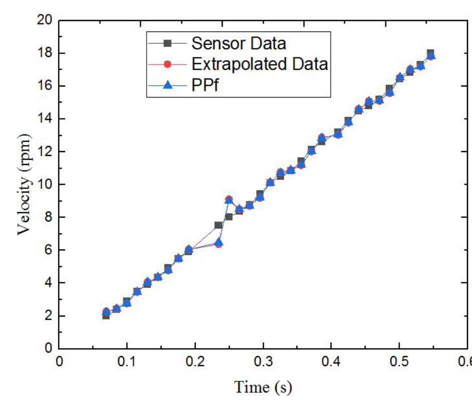

Fig. 6. 100-rpm velocity sensor data with extrapolated and PPF values.

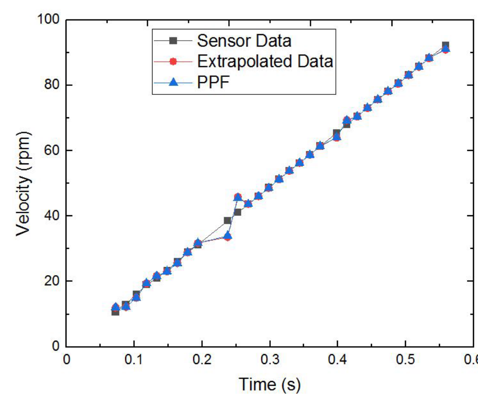

Fig. 7. 500-rpm velocity sensor data with extrapolated and PPF values.

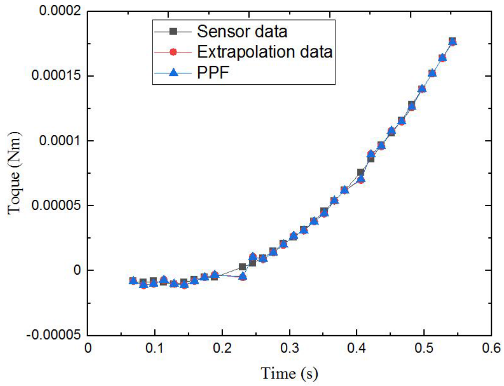

Fig. 8. Predicted value of disturbance torque (PPF), extrapolated values, and sensor data at 50-rpm velocity.

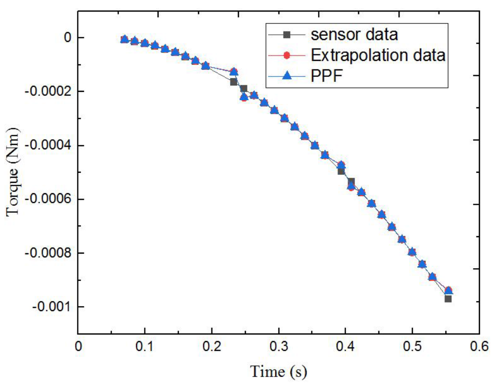

Fig. 9. Predicted value of disturbance torque (PPF), extrapolated values, and sensor data at −50-rpm velocity.

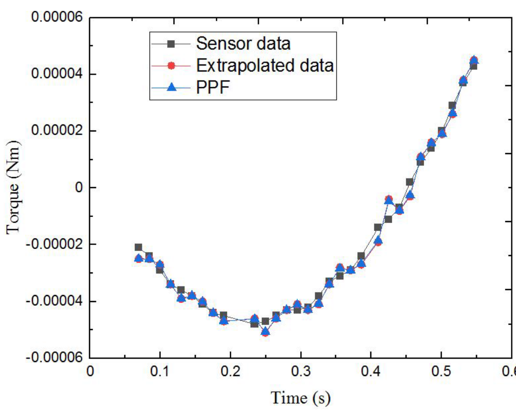

Fig. 10. Predicted value of disturbance torque (PPF), extrapolated values, and sensor data at 100-rpm velocity.

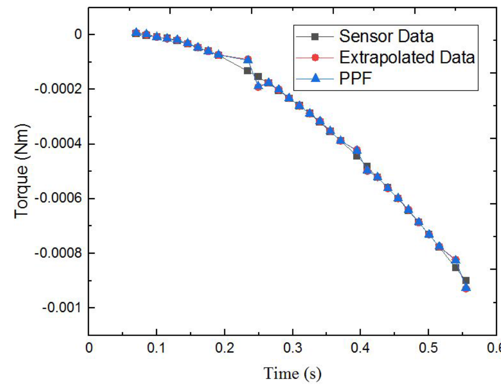

Fig. 11. Predicted value of disturbance torque (PPF), extrapolated values, and sensor data at −100-rpm velocity.

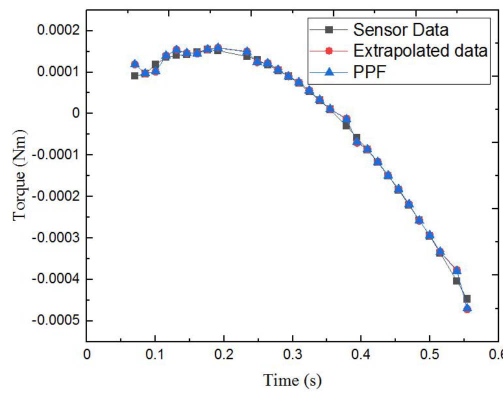

Fig. 12. Predicted value of disturbance torque (PPF), extrapolated values, and sensor data at 500-rpm velocity.

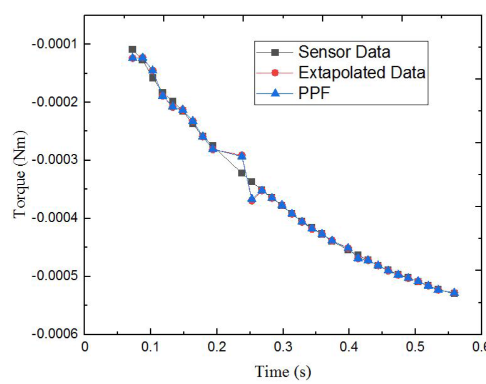

Fig. 13. Predicted value of disturbance torque (PPF), extrapolated values, and sensor data at −500-rpm velocity.

TABLE V
SMALL DC MOTOR SPECIFICATIONS

Specification of motors	
Manufacturer	Electrocraft
Version	Series 116-4
Maximum Terminal Voltage	24V DC
Supply Voltage	12V DC
Peak Torque	6 Nm
Maximum Speed	3200 rpm

Figs. 8–13 illustrate the graphic summary of the relationship between the sensor data, the extrapolated value, and the PPF value of the disturbance torque. The horizontal axis describes the time, while the vertical axis highlights the disturbance torque, which manifests a strong association between sensor data and extrapolated values of disturbance torque. It can be seen that sensor data and PPF values are very close to each other, and it is negligible ($\sigma = 1.83 \times 10^{-6}$). Fig. 10 of the 100-rpm velocity has some nonlinearities even though our filters predict the value with a standard deviation of ($\sigma = 1.80 \times 10^{-6}$).

Figures 5–13 depict convincing evidence for a strong association between PPF and DOB data. PPF provides an algo-

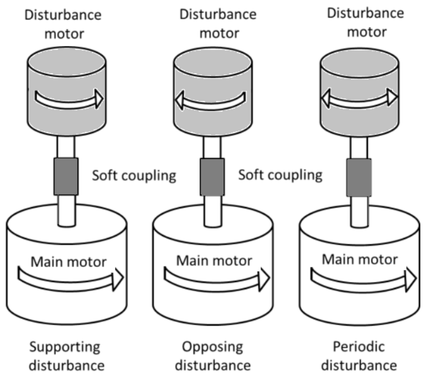

Fig. 14. Different types of disturbances are applied to the dc motor.

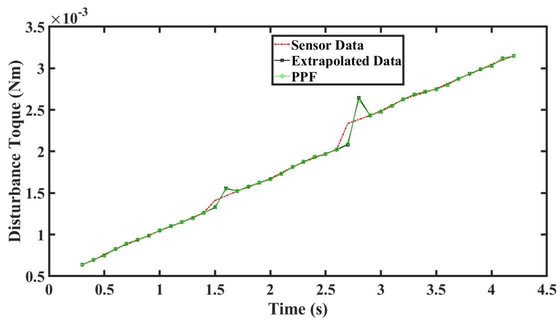

Fig. 15. Supporting disturbance estimated from 40 sample data.

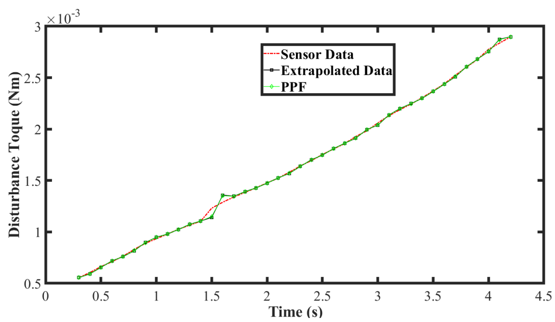

Fig. 16. Opposing disturbance estimated from 40 sample data.

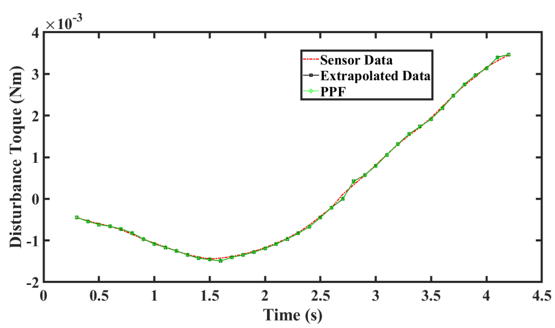

Fig. 17. Periodic disturbance estimated from 40 sample data.

rithm to determine an estimate by combining models of the system and noisy measurements of certain parameters using polynomial extrapolation. Thus, the data from the DOB can fit into polynomial equations and extrapolate the future value according to the degree of the polynomial that matches the

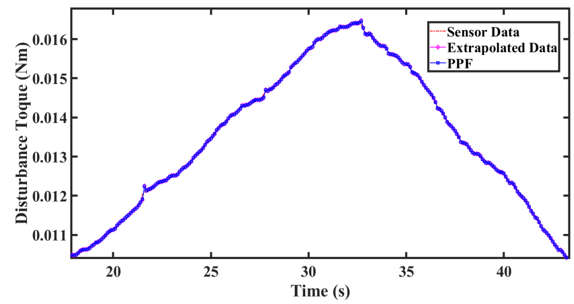

Fig. 18. Overall system performance of the PPF with supporting disturbance.

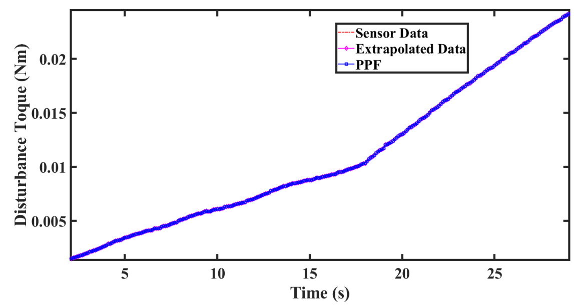

Fig. 19. Overall system performance of the PPF with opposing disturbance.

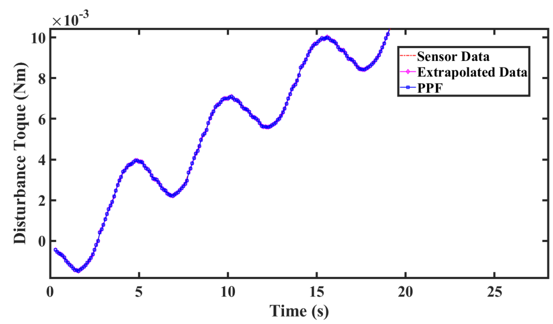

Fig. 20. Overall system performance of the PPF with periodic disturbance.

polynomial equation. However, convergence can only be guaranteed for linearized systems. State estimation for nonlinear systems is the subject of this work; therefore, the convergence of the original nonlinear system must be verified and validated.

To validate the PPF-based DOB data experimentally, the experimental setup is described in Fig. 14. When estimating the dynamic state in nonlinear situations, we consider that external disturbances can be applied using different small dc motors with different modes. To reduce the gravitational influence of the connected motor, motor shafts were coupled, and the disturbance motor was placed on top of the main motor. There are three methods to apply disturbances: supporting, opposing, and periodic. The controller of the disturbance motor uses a constant PWM to produce applied disturbances in the supporting and opposing modes. In the periodic disturbance mode, a constant sinusoidal disturbance with a range of frequencies was delivered. The arrows in Fig. 14 represent the rotational direction of the motors in each mode. Table V presents the small dc motor specifications of the experimental system.

The disturbance torque estimated and predicted using the sensor and the PPF values for the three types of disturbances of the 40 data points are plotted against time, as shown in Figs. 15–17, and Figs. 18–20 show the overall performance of the PPF with sensor values. From the three types of disturbances applied to the system for validating the nonlinear scenario, the figures show that the PPF can achieve optimized prediction and estimation of nonlinear states.

There was a statistically significant correlation between the proposed method and a previous study based on the observer-based dc motor parameter estimation method [1], [11], [44]. These findings demonstrated the effectiveness of the proposed method. Further validation studies using the existing estimation methods are required. This aspect should be considered in future studies.

V. Conclusion

To achieve the desired responses in motion control applications, predicting and compensating for the states and noise are essential to increase the robustness, high precision, and fast responses of the system. In this study, a novel PPF method was proposed for estimating the states from consecutive and evenly spaced sensor data with noise using polynomial extrapolation. With this approach, computational expenses can be minimized, and small nonlinearities and the related mathematical burden can be reduced by employing a suitably precise low-order polynomial approximation. In parallel, we proved that the DOB can be converted into an estimator and predictor to calculate the disturbance torque in dc motor systems. The algorithm operates in three stages: initialization, which provides the initial system state, and initial state uncertainty, which is followed by the prediction. To experimentally validate the algorithm, the velocity response, the motor torque, and the disturbance torque of the dc motor were measured. PPF approximates the data from the motor drives and estimates the value of $\hat{z}_n$ based on previous measurements from the DOB. The difference between the real-time DOB data and PPF-based predicted values shows a standard deviation of 0.12624 for the velocity component and 2.02×10^{-6} for the disturbance torque. From the performance analysis of the proposed method combined with the previous study method, a statistically significant relationship can be observed. The validity of the proposed method is experimentally verified. Further validation of the prediction method should be performed using other existing methods.

References

[1] B. M. Pillai and J. Suthakorn, "Motion control applications: Observer based DC motor parameters estimation for novices," *Int. J. Power Electron. Drive Syst.*, vol. 10, no. 1, pp. 195–210, Mar. 2019.

[2] W. P. N. dos Reis and O. Morandin Jr., "Sensors applied to automated guided vehicle position control: A systematic literature review," *Int. J. Adv. Manuf. Technol.*, vol. 113, nos. 1–2, pp. 21–34, Mar. 2021.

[3] L. Wang, X. V. Wang, J. Váncza, and Z. Kemény, *Advanced Human-Robot Collaboration in Manufacturing*. Cham, Switzerland: Springer, 2021.

[4] K. Ohnishi, M. Shibata, and T. Murakami, "Motion control for advanced mechatronics," *IEEE/ASME Trans. Mechatron.*, vol. 1, no. 1, pp. 56–67, Mar. 1996.

[5] J. Yadav and J. Suthakorn, "Euclidean distance and workspace region based control algorithm for collision avoidance in a laparoscopic surgical robot: MU-LapaRobot," in *Proc. IEEE Int. Conf. Robot. Biomimetics (ROBIO)*, Dec. 2012, pp. 2056–2061.

[6] S. Liu, L. Wang, and X. V. Wang, "Sensorless force estimation for industrial robots using disturbance observer and neural learning of friction approximation," *Robot. Comput.-Integr. Manuf.*, vol. 71, Oct. 2021, Art. no. 102168.

[7] A. H. S. Abeykoon and M. B. Pillai, "RTOS based embedded controller implementation of a bilateral control system," *J. Nat. Sci. Found. Sri Lanka*, vol. 42, no. 3, p. 217, Sep. 2014.

[8] S. Ding, W. Chen, K. Mei, and D. J. Murray-Smith, "Disturbance observer design for nonlinear systems represented by input–output models," *IEEE Trans. Ind. Electron.*, vol. 67, no. 2, pp. 1222–1232, Feb. 2020.

[9] E. Sariyildiz, R. Oboe, and K. Ohnishi, "Disturbance observer-based robust control and its applications: 35th anniversary overview," *IEEE Trans. Ind. Electron.*, vol. 67, no. 3, pp. 2042–2053, Mar. 2020.

[10] S. Shimmyo, "Multilevel motor drives for robust motion control," Ph.D. dissertation, Dept. Syst. Des. Eng., Keio Univ., Tokyo, Japan, 2016.

[11] B. M. Pillai, D. Sivaraman, S. Ongwattanakul, and J. Suthakorn, "Sensorless based gravity torque estimation and friction compensation for surgical robotic system," in *Proc. IEEE 9th Int. Conf. e-Learn. Ind. Electron. (ICELIE)*, Oct. 2022, pp. 1–6.

[12] W.-H. Chen, J. Yang, L. Guo, and S. Li, "Disturbance-observer-based control and related methods—An overview," *IEEE Trans. Ind. Electron.*, vol. 63, no. 2, pp. 1083–1095, Feb. 2016.

[13] A. M. H. S. Abeykoon and K. Ohnishi, "Bilateral control interacting with a virtual model and environment," in *Proc. IEEE Int. Conf. Ind. Technol.*, Dec. 2006, pp. 1320–1325.

[14] F. V. Van Breugel, J. N. Kutz, and B. W. Brunton, "Numerical differentiation of noisy data: A unifying multi-objective optimization framework," *IEEE Access*, vol. 8, pp. 196865–196877, 2020.

[15] S. Park, M. Gil, H. Im, and Y. Moon, "Measurement noise recommendation for efficient Kalman filtering over a large amount of sensor data," *Sensors*, vol. 19, no. 5, p. 1168, 2019.

[16] G. D. Cormack and J. N. McMullin, "Frequency de-aliased FFT analysis of step-like functions," *IEEE Trans. Instrum. Meas.*, vol. 40, no. 4, pp. 773–775, Aug. 1991.

[17] T. I. Laakso and S. J. Ovaska, "Prefiltering approach for optimal polynomial prediction," *IEEE Trans. Signal Process.*, vol. 44, no. 3, pp. 701–705, Mar. 1996.

[18] J. M. D. C. Sousa and M. Setnes, "Fuzzy predictive filters in model predictive control," *IEEE Trans. Ind. Electron.*, vol. 46, no. 6, pp. 1225–1232, Dec. 1999.

[19] O. Vainio and S. J. Ovaska, "A class of predictive analog filters for sensor signal processing and control instrumentation," *IEEE Trans. Ind. Electron.*, vol. 44, no. 4, pp. 565–570, Aug. 1997.

[20] O. Vainio and S. J. Ovaska, "Noise reduction in zero crossing detection by predictive digital filtering," *IEEE Trans. Ind. Electron.*, vol. 42, no. 1, pp. 58–62, Feb. 1995.

[21] J. H. Painter, D. Kerstetter, and S. Jowers, "Reconciling steady-state Kalman and alpha-beta filter design," 1990.

[22] M. Grewal and A. P. Andrews, *Kalman Filtering. Theory and Practice* (Information and System Sciences Series T). Upper Saddle River, NJ, USA: Prentice-Hall, 1993.

[23] J.-B. Lacambre, M. Narozny, and J.-M. Louge, "Limitations of the unscented Kalman filter for the attitude determination on an inertial navigation system," in *Proc. IEEE Digit. Signal Process. Signal Process. Educ. Meeting (DSP/SPE)*, Aug. 2013, pp. 187–192.

[24] F. Beltran-Carbajal, A. Valderrabano-Gonzalez, J. C. Rosas-Caro, and A. Favela-Contreras, "An asymptotic differentiation approach of signals in velocity tracking control of DC motors," *Electr. Power Syst. Res.*, vol. 122, pp. 218–223, May 2015.

[25] O. A. Stepanov, V. A. Vasiliev, M. V. Basin, V. A. Tupysev, and Y. A. Litvinenko, "Application of polynomial filtering algorithms to nonlinear discrete dynamical systems in navigation data processing," in *Proc. Eur. Control Conf. (ECC)*, May 2020, pp. 1751–1756.

[26] M. Hernandez-Gonzalez and M. V. Basin, "Discrete-time filtering for nonlinear polynomial systems over linear observations," in *Proc. Amer. Control Conf.*, Jun. 2014, pp. 2273–2278.

[27] F. Gheorghiu and C. S. Williams, *Designing Digital Filters: Solutions Manual*. Upper Saddle River, NJ, USA: Prentice-Hall, 1986.

[28] S. Valiviita, S. J. Ovaska, and O. Vainio, "Polynomial predictive filtering in control instrumentation: A review," *IEEE Trans. Ind. Electron.*, vol. 46, no. 5, pp. 876–888, Oct. 1999.

[29] S. J. Ovaska, "Improving the velocity sensing resolution of pulse encoders by FIR prediction," *IEEE Trans. Instrum. Meas.*, vol. 40, no. 3, pp. 657–658, Jun. 1991.

[30] J. Pasanen, O. Vainio, and S. J. Ovaska, "Predictive synchronization and restoration of corrupted velocity samples," *Measurement*, vol. 13, no. 4, pp. 315–324, Jul. 1994.

[31] S. Valiviita and O. Vainio, "Delayless differentiation algorithm and its efficient implementation for motion control applications," *IEEE Trans. Instrum. Meas.*, vol. 48, no. 5, pp. 967–971, Oct. 1999.

[32] S. J. Ovaska and S. Valiviita, "Angular acceleration measurement: A review," in *Proc. IMTC IEEE Instrum. Meas. Technol. Conf. Where Instrum. Going*, vol. 2, May 1998, pp. 875–880.

[33] N. Wiener, N. Wiener, C. Mathematician, N. Wiener, N. Wiener, and C. Mathématicien, *Extrapolation, Interpolation, and Smoothing of Stationary Time Series: With Engineering Applications*, vol. 113, no. 21. Cambridge, MA, USA: MIT Press, 1949.

[34] R. E. Kalman, "A new approach to linear filtering and prediction problems," *Trans. ASME-J. Basic Eng.*, vol. 82, pp. 35–45, 1960.

[35] S. Mirjalili, "Genetic algorithm," in *Evolutionary Algorithms and Neural Networks*. Cham, Switzerland: Springer, 2019, pp. 43–55.

[36] S. Brooks, A. Gelman, G. Jones, and X.-L. Meng, *Handbook Markov Chain Monte Carlo*. Boca Raton, FL, USA: CRC Press, 2011.

[37] S. J. Ovaska, "Newton-type predictors—A signal processing oriented viewpoint," *Signal Process.*, vol. 25, no. 2, pp. 251–257, Nov. 1991.

[38] D. Morgan and A. Aridgides, "Interpolation and extrapolation of an ideal band-limited random process," *IEEE Trans. Acoust., Speech, Signal Process.*, vol. ASSP-35, no. 1, pp. 43–47, Jan. 1987.

[39] N. Morrison, "Tracking filter engineering: The Gauss–Newton and polynomial filters-supplementary materia and errata," Inst. Eng. Technol., South Afr. Dept. Defence, South Africa, Tech. Rep., Dec. 2012, doi: 10.1049/PBRA023E.

[40] Y. Pei, S. Biswas, D. S. Fussell, and K. Pingali, "An elementary introduction to Kalman filtering," *Commun. ACM*, vol. 62, no. 11, pp. 122–133, Oct. 2019.

[41] M. Loève, "Graduate texts in mathematics," in *Probability Theory I*, vol. 45, 4th ed. Springer, Jun. 2012, pp. 159–160.

[42] X.-B. Jin, R. J. R. Jeremiah, T.-L. Su, Y.-T. Bai, and J.-L. Kong, "The new trend of state estimation: From model-driven to hybrid-driven methods," *Sensors*, vol. 21, no. 6, p. 2085, Mar. 2021.

[43] S. Nakdhamabhorn, M. B. Pillai, and J. Suthakorn, "Design and development of sensorless based 5-DOF bilaterally controlled surgical manipulator: A prototype," *Bull. Electr. Eng. Informat.*, vol. 10, no. 2, pp. 619–631, Apr. 2021.

[44] H. R. Senevirathne, A. M. H. S. Abeykoon, and M. B. Pillai, "Disturbance rejection analysis of a disturbance observer based velocity controller," in *Proc. IEEE 6th Int. Conf. Inf. Autom. Sustainability*, Sep. 2012, pp. 59–64.

Dileep Sivaraman (Graduate Student Member, IEEE) received the integrated master's degree in physics from Amrita Vishwa Vidyapeetham University, Coimbatore, India, in 2012. He is currently pursuing the Ph.D. degree in biomedical engineering (medical robotics) with the Center for Biomedical and Robotics Technology (BART LAB), Faculty of Engineering, Mahidol University, Nakhon Pathom, Thailand.

He has been involved with research pertaining to advanced motion control, sensor fusion, medical robotics, bioimage processing, and rescue robotics along the direction of dynamics and control.

Songpol Ongwattanakul (Member, IEEE) received the bachelor's degree in computer engineering from the King Mongkut's University of Technology Thonburi, Bangkok, Thailand, in 1994, the master's degree in computer science from The University of Edinburgh, Edinburgh, Scotland, U.K., in 1997, and the Ph.D. degree in electrical engineering from The University of Alabama, Tuscaloosa, AL, USA, in 2003.

He is currently the Executive Director of the Center for Biomedical and Robotics Technology (BART LAB), Mahidol University, Nakhon Pathom, Thailand, where he is also the Director of the Biomedical Cloud Computing Laboratory. His research interest is aimed toward cloud computing in the healthcare industry and healthcare information systems' big data in healthcare.

Jackrit Suthakorn (Member, IEEE) received the bachelor's degree in mechanical engineering from Mahidol University, Nakhon Pathom, Thailand, in 1995, the master's degree in control engineering from Michigan Technological University, Houghton, MI, USA, in 1998, and the Ph.D. degree in robotics from Johns Hopkins University, Baltimore, MD, USA, in 2003.

He established the Center for Biomedical and Robotics Technology (BART LAB), the first interdisciplinary research laboratory in the Faculty of Engineering, Mahidol University, in 2004. In 2006, he and his colleagues established the Department of Biomedical Engineering at Mahidol University, where he was the first BME Department Chair and remained until 2015. Since 2015, he has been the Dean of the Faculty of Engineering, Mahidol University. He is currently the President leading the Council of Engineering Deans of Thailand. His research interest is aimed toward medical robotics and field robotics: surgical robotics in various applications, rehabilitation robotics, hospital service and telemedicine robotics, and rough terrain rescue robotics.

Dr. Suthakorn was one of the founders of the Thai Robotics Society (TRS) in 2004 and the President from 2007 to 2010. He also serves as a Trustee of the International RoboCup Federation and the Vice-President of RoboCup Asia-Pacific (RCAP).

Branesh M. Pillai (Member, IEEE) received the bachelor's degree from Anna University, Chennai, India, in 2007, the master's by research degree in control systems from the University of Moratuwa, Moratuwa, Sri Lanka, in 2013, and the Ph.D. degree in biomedical engineering (medical robotics) from Mahidol University, Nakhon Pathom, Thailand, in 2019.

He is currently a Faculty Member of the Center for Biomedical and Robotics Technology (BART LAB), Faculty of Engineering, Mahidol University. His main fields of expertise include medical robotics and the work-related to advanced motion control, robot-assisted surgery, and biomechanics. Rough terrain rescue robot is the area of his interest systems.